Mechanics of Materials 92 (2016) 155–163

Contents lists available at ScienceDirect

Mechanics of Materials

journal homepage: www.elsevier.com/locate/mechmat

Adhesive impact of an elastic sphere with an elastic half space: Numerical analysis based on the method of dimensionality reduction

I.A. Lyashenko[a,b], E. Willert[b], V.L. Popov[b,c,d,*]

[a] Sumy State University, 40007 Sumy, Ukraine
[b] Berlin University of Technology, 10623 Berlin, Germany
[c] National Research Tomsk State University, 634050 Tomsk, Russia
[d] National Research Tomsk Polytechnic University, 634050 Tomsk, Russia

ARTICLE INFO

Article history:
Received 23 August 2015
Revised 10 September 2015
Available online 16 September 2015

Keywords:
Plain impacts
JKR–adhesion
No-Slip
Elastic spheres
Method of dimensionality reduction

ABSTRACT

An impact of an elastic sphere with an elastic half space in the presence of adhesion is studied numerically using the method of dimensionality reduction. It is shown that the rebound velocities and angular velocity, written in proper dimensionless variables, are determined by a function of only the ratio of tangential and normal stiffness ("Mindlin-ratio") and one further parameter describing the adhesion properties of the contact. The obtained numerical results can be approximated by analytical expressions.

1. Introduction

Impacts of solid particles are of interest for many physical and technological processes related to the dynamics of granular media (Thornton and Yin, 1991; Ciamarra et al., 2004; Jop et al., 2006; Brilliantov et al., 1996). Even for spherical particles from purely elastic material, the detailed dynamics of the impact can be very complicated.

However, the problem formulation can be simplified by using the Method of Dimensionality Reduction (MDR) (Popov and Psakhie, 2007; Popov; 2013; Popov and Heß, 2014, 2015). In the MDR, the contact problem of a particle with a half space is replaced by a contact of a plain indenter of properly modified profile shape with a linear elastic foundation consisting of independent springs. This simplifies the contact problem drastically and opens new ways for analytical and numerical treatment of dynamic normal and tangential contacts.

In the recent publication (Lyashenko and Popov, 2015) an impact of an elastic sphere with an elastic half space under no-slip conditions was studied numerically using the MDR. It was shown that the rebound velocity and angular velocity, written in proper dimensionless variables, are determined by a function of only the ratio of tangential and normal stiffness ("Mindlin-ratio"). However, in many real situations, for example powder technologies or in biological systems, the contact force between particles during their interactions has adhesive contribution. In the present paper, the solution obtained in Lyashenko and Popov (2015) will be extended to the case of adhesive impacts, under the same assumptions as in the theory by Johnson, Kendall and Roberts in Johnson et al. (1971), known as JKR – theory.

In the experimental work by Waters and Guduru (2009), it has been shown that normal and tangential contributions to adhesion forces may depend on the direction of the

* Corresponding author at: Technische Universität Berlin, Institut für Mechanik, FG Systemdynamik und Reibungsphysik, Sekr. C8-4, Raum M 122, Straße des 17. Juni 135, 10623 Berlin, Germany. Tel.: +49 (0)30/314-21480.
E-mail address: v.popov@tu-berlin.de (V.L. Popov).

http://dx.doi.org/10.1016/j.mechmat.2015.09.009
0167-6636/

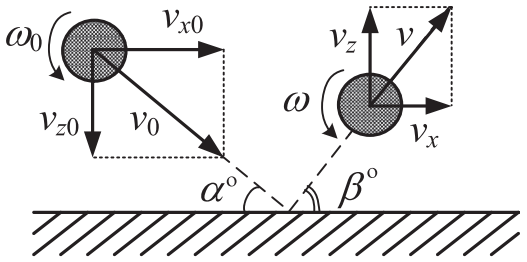

Fig. 1. Schematic representation of an impact.

motion of the particle. In this paper we assume conditions under which the influence of tangential loading on the adhesion in the normal direction can be neglected. In this case we can describe the influence of adhesion by a standard procedure within the framework of the MDR (Popov and Heß, 2014). Kosinski and Hoffmann (2011) studied the influence of adhesion in Lagrangian particle-fluid flows using the JKR – theory. They gave dimensionless formulations and comprehensive solutions for a wide parameter space in the case of a pure normal adhesive impact. (Ledvinkova and Kosek (2013) used discrete element method (DEM) to study impacts between polymer particles, which they modeled as agglomerations of elastic microelements bound by adhesive forces. They focused on impact times and the processes of agglomeration and disintegration of the polymer particles during the impact. The impact problem for the adhesive normal contact was studied analytically and experimentally by Andres (1995). He thereby applied the adhesion models of Johnson et al. (JKR – theory), Deryagin et al. (DMT – theory) and Maugis. A comprehensive analytical model of the adhesive normal contact impact problem using the JKR – theory was derived by Brilliantov et al. (2007). The oblique impact without adhesion was studied in a series of papers by Maw et al. (1976, 1977, 1981). To our knowledge no efforts have been published yet to address the oblique adhesive impact problem.

The paper is organized as follows. In Section 2, we first give the problem formulation and after that in Section 3 reproduce, as a basis for further consideration, the classical solution for an impact without adhesion based on the assumption of rigid rotation at the last moment of contact. We then solve a simplified model with adhesion under assumption of constant contact stiffness. This derivation provides the general form of the solution and the main dimensionless parameters which will play a role in the subsequent rigorous simulation. In Section 4, the numerical model of the impact problem based on the MDR is presented, the results of which are described in Section 5 and compared with experimental results for the normal adhesive contact in Section 6. The final Section 7 concludes the paper.

2. Problem formulation and assumptions

Let us consider an impact of an elastic sphere with mass m and radius R on an elastic half space, as shown in Fig. 1. Let the moduli of elasticity of the sphere and the half space be E_1 and E_2, their Poison's numbers ν_1 and ν_2, and their shear moduli G_1 and G_2, accordingly. We will restrict ourselves to the case of elastically similar media, i.e.

$$\frac{1-2\nu_1}{G_1} = \frac{1-2\nu_2}{G_2}, \tag{1}$$

for which the tangential and normal contact problem will decouple. We will work within the half space approximation, so the indentation depth is always assumed to be small compared to the contact radius. Moreover all lengths associated with the contact are considered negligible compared to the sphere radius R. We assume that the adhesion in the contact can be described by the JKT-type theory in spite of the fact that no-slip condition is assumed in the whole contact. Note, that it was shown by Borodich et al. (2012) that in the case of intermolecular attraction the assumption of no-slip is physically more appropriate than the one of no shear stresses in the contact, usually used within the JKR – theory. However, in the case of elastic similar materials satisfying Eq. (1), there is no difference between the frictionless and no-slip normal contact. And even in the case of materials which do not satisfy (1), the following theory can be used in a very good approximation as the difference of the results of an adhesive contact with and without sliding in the contact interface is of the same order of magnitude as the difference of normal stiffness of a cylindrical indenter with and without friction, which for Poisson numbers between 0.3 and 0.5 does not exceed 3% (Borodich et al., 2012).

We will also assume a quasi-static impact, i.e. impact velocities being much smaller than the velocity of sound in the elastic half space. In this case the inertia of the half space is negligible. The loss of kinetic energy during the impact due to elastic waves propagating into the half space (Hunter, 1957) is neglected.

The main notations are illustrated in Fig. 1: The incident velocity of the center of mass of the sphere is v_0 with horizontal and vertical components v_{x0} and v_{z0}, the incident angular velocity ω_0, the rebound velocity is v with components v_x and $-v_z$, the grazing angle is α°, and the rebound angle β°.

3. A linear model of the oblique adhesive impact without slip

Let F_x and F_z be the components of the contact force acting on the sphere during the impact. The equations of motion of the sphere in the integral form can be written as

$$m(v_z - v_{z0}) = -\int_0^t F_z(t')\mathrm{d}t', \tag{2}$$

$$m(v_x - v_{x0}) = -\int_0^t F_x(t')\mathrm{d}t', \tag{3}$$

$$I(\omega - \omega_0) = -R\int_0^t F_x(t')\mathrm{d}t', \tag{4}$$

where t denotes the duration of the impact and $I = (2/5)mR^2$ is the moment of inertia of the sphere. We first reproduce the classical text-book solution of the impact problem. Together with the rolling condition for the tangential rebound velocity,

$$v_x + \omega R = 0, \tag{5}$$

Eqs. (2)–(4) determine unambiguously all kinematic quantities of the sphere after the impact:

$$\bar{v}_x = \frac{5}{7}v_{x0} - \frac{2}{7}R\omega_0, \tag{6}$$

$$\bar{\omega} = \frac{2}{7}\omega_0 - \frac{5}{7}\frac{v_{x0}}{R}. \tag{7}$$

It can be seen easily that the impact is non-elastic, as the energy change during the impact,

$$\Delta E = \frac{m}{2}(\bar{v}_x^2 - v_{x0}^2) + \frac{I}{2}(\bar{\omega}^2 - \omega_0^2) = -\frac{m}{7}(v_{x0} + R\omega_0)^2 \tag{8}$$

is negative. This solution is, however, oversimplified. While Eqs. (2)–(4) are exact (under the assumption of very short impact time), the kinematic condition (5) is intrinsically controversial: it cannot be valid during the whole time of impact, and its application to the last moment of impact is an arbitrary and not substantiated assumption. In reality, due to the elasticity of the sphere, the condition (5) will be valid *only* at one point in time during the impact.

In a second step let us take into account the normal and tangential compliance of the contact in a simplified way. The normal and tangential compliance of the contact are changing during the impact due to changing contact configuration. Let us simplify this situation by considering an impact of a rigid sphere having a linear spring with normal and tangential stiffness in the contact region. This could also be an elastic sphere with a flat patch. Due to the flat patch the contact stiffness will be constant provided the contact radius does not change considerably during the impact. The contact forces will then be given by

$$F_N = k_z u_z, \tag{9}$$

$$F_f = k_x(u_x + R\varphi). \tag{10}$$

In the last equation we took into account the fact that, due to the assumption of no slip in the contact, the tangential displacement of the contact point is the sum of the displacement of the center of mass and the displacement due to rigid rotation. The solution of the set of Eqs. (2)–(4, 9, 10) with the initial conditions

$$\begin{aligned} &u_x(0) = 0,\ \dot{u}_x(0) = v_{x0}, u_z(0) = 0, \dot{u}_z(0) = v_{z0},\\ &\varphi(0) = 0, \dot{\varphi}(0) = \omega_0 \end{aligned} \tag{11}$$

has the form

$$\dot{u}_z(t) = v_{z0}\cos(\omega_z t), \tag{12}$$

$$\dot{u}_x(t) = \left(\frac{5}{7}v_{x0} - \frac{2}{7}R\omega_0\right) + \frac{2}{7}(v_{x0} + R\omega_0)\cos(\omega_x t), \tag{13}$$

$$\dot{\varphi}(t) = \left(\frac{2}{7}\omega_0 - \frac{5}{7}\frac{v_{x0}}{R}\right) + \frac{5}{7R}(v_{x0} + R\omega_0)\cos(\omega_x t), \tag{14}$$

where $\omega_z = \sqrt{k_z/m}$, and $\omega_x = \sqrt{7k_x/(2m)}$. We now characterize adhesion by the maximum "negative indentation depth" $-d_c$ at which the adhesive contact loses stability and the contact is lost. The moment of the detachment t_i can be obtained from the solution for the vertical motion (12):

$$u_z(t_i) = \frac{v_{z0}}{\omega_z}\sin(\omega_z t_i) = -d_c. \tag{15}$$

We find:

$$t_i = \frac{1}{\omega_z}\arcsin\left(\frac{-d_c\omega_z}{v_{z0}}\right) = \frac{1}{\omega_z}\left[\pi + \arcsin\left(\frac{d_c\omega_z}{v_{z0}}\right)\right]. \tag{16}$$

The velocities at the last moment of the impact are equal to

$$v_z = \dot{u}_z(t_i) = -v_{z0}\sqrt{1 - \left(\frac{d_c\omega_z}{v_{z0}}\right)^2} = -v_{z0}\sqrt{1-\beta^2}, \tag{17}$$

$$\begin{aligned} v_x = \dot{u}_x(t_i) &= \overbrace{\left(\frac{5}{7}v_{x0} - \frac{2}{7}R\omega_0\right)}^{\bar{v}_x} + \frac{2}{7}\overbrace{(v_{x0} + R\omega_0)}^{V}\\ &\quad\times\cos\overbrace{\left[\sqrt{\frac{7}{2}\frac{k_x}{k_z}}\left(\pi + \arcsin\left(\frac{d_c\omega_z}{v_{z0}}\right)\right)\right]}^{\phi}\\ &= \bar{v}_x + \frac{2}{7}V\cos[\phi(\gamma,\beta)], \end{aligned} \tag{18}$$

$$\omega = \dot{\varphi}(t_i) = \bar{\omega} + \frac{5}{7R}V\cos[\phi(\gamma,\beta)], \tag{19}$$

with $\beta = d_c\omega_z/v_{z0}$ and $\gamma = \sqrt{\frac{7}{2}\frac{k_x}{k_z}}$. Note that the expressions for $\bar{v}_x$ and $\bar{\omega}$ are exactly the classical solutions (6) and (7), while the remainder of (18) and (19) describes the influence of the finite tangential compliance. Let us determine the loss of energy during the impact. It is convenient to consider the kinetic energies of horizontal and vertical motion separately:

$$\Delta E_x = -\frac{m}{7}(v_{x0} + R\omega_0)^2\sin^2[\phi(\gamma,\beta)], \tag{20}$$

$$\Delta E_z = -\frac{mv_{z0}^2}{2}\beta^2 = -E_{z0}\beta^2. \tag{21}$$

Eqs. (17)–(21) can be rewritten in the following way:

$$\frac{v_z}{v_{z0}} = -\sqrt{1-\beta^2}, \tag{22}$$

$$\frac{\Delta E_z}{E_{z0}} = -\beta^2, \tag{23}$$

$$\frac{7}{2}\frac{v_x - \bar{v}_x}{V} = \frac{7}{5}\frac{R(\omega - \bar{\omega})}{V} = \cos[\phi(\gamma,\beta)], \tag{24}$$

$$\frac{7\Delta E_x}{m(v_{x0} + R\omega_0)^2} = -\sin^2[\phi(\gamma,\beta)]. \tag{25}$$

The expressions on the right side are functions only of the stiffness ratio k_x/k_z and the displacement ratio

$$\beta = \frac{d_c\omega_z}{v_{z0}} = \frac{d_c}{d}, \tag{26}$$

where d denotes the maximum indentation depth (in the case of constant stiffness the maximum indentation depth is the same with and without adhesion, in the more general case we will assume d to be the corresponding indentation depth for an impact without adhesion).

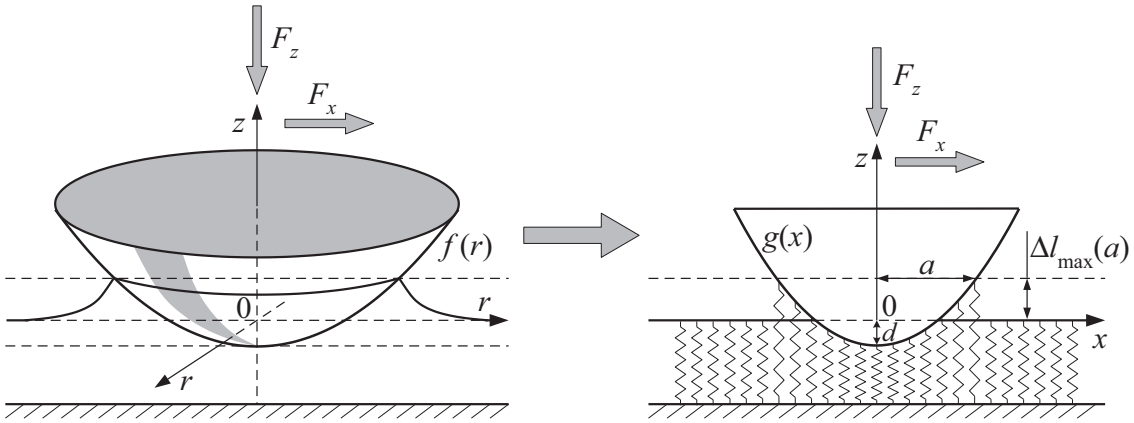

Fig. 2. MDR transformation of the original three-dimensional profile into one-dimensional image and replacement of the elastic half-space by an elastic foundation.

Note, that for an arbitrary rotationally symmetric body the ratio of differential tangential and normal stiffness is constant and equal to $k_x/k_z = G^*/E^*$ with the effective moduli

$$\frac{1}{E^*} = \frac{1-\nu_1^2}{E_1} + \frac{1-\nu_2^2}{E_2}, \tag{27}$$

$$\frac{1}{G^*} = \frac{2-\nu_1}{4G_1} + \frac{2-\nu_2}{4G_2}. \tag{28}$$

In Campañá et al. (2011) and Grzemba et al. (2014) it was shown by numerical simulations that this is valid even for randomly rough fractal surfaces. We thus may anticipate that in the general case (for example of impact of a sphere with an elastic half-space) the relations given above have to be replaced by

$$\frac{7}{2}\frac{v_x - \tilde{v}_x}{V} = \frac{7}{5}\frac{R(\omega-\tilde{\omega})}{V} = P(\gamma,\beta), \tag{29}$$

$$\frac{7\Delta E_x}{m(v_{x0}+R\omega_0)^2} = -1 + (P(\gamma,\beta))^2, \tag{30}$$

$$\frac{v_z}{v_{z0}} = -F(\beta), \tag{31}$$

$$\frac{\Delta E_z}{E_{z0}} = -1 + (F(\beta))^2 \tag{32}$$

with

$$\gamma = \sqrt{\frac{7}{2}\frac{G^*}{E^*}}. \tag{33}$$

Let us derive the equation for the dimensionless parameter describing the adhesion in the case of impact of a sphere with an elastic half-space. The maximum indentation depth d (for the non-adhesive contact) is given by the theory of Hertz (1881)

$$d = \left(\frac{15}{16}\frac{mv_{z0}^2}{E^* R^{1/2}}\right)^{2/5} \tag{34}$$

and the maximum displacement in the moment of detachment of the adhesive contact by the JKR – theory (Johnson et al., 1971):

$$d_c = \frac{3}{4}\left(\frac{\pi^2 R\Delta\gamma^2}{E^{*2}}\right)^{1/3}, \tag{35}$$

where $\Delta\gamma$ it is the surface energy. Hence, we arrive at

$$\beta = \pi^{2/3}\frac{3}{4}\left(\frac{16}{15}\right)^{2/5}\frac{R^{8/15}\Delta\gamma^{2/3}}{E^{*4/15}m^{2/5}v_{z0}^{4/5}}. \tag{36}$$

For convenience and simplicity we will omit the constant and write

$$\beta = \left(\frac{R^4\Delta\gamma^5}{E^{*2}m^3v_{z0}^6}\right)^{2/15}. \tag{37}$$

In Sections 4 and 5, we will prove the hypothesis given by Eqs. (29)–(32) by numerical simulations and find the form of the functions $P(\gamma,\beta)$ and $F(\beta)$, which constitute the solution of the impact problem.

The results obtained above could be generalized for an arbitrary rigid indenter of parabolic shape in the vicinity of the contact. This would introduce two more parameters, first a non-dimensional radius of gyration $K = \sqrt{I/(MR^2)}$ (Maw et al., 1976) and second an alignment angle Φ between the normal axis of the half space and the axis between the point of contact and the center of mass. However, we will restrict ourselves to the case of a homogeneous sphere, i.e. $K = \sqrt{0.4}$ and $\Phi = 0$ to be able to show a comprehensive solution of the studied problem.

4. Impact of a sphere with account of normal adhesion: numerical model based on the MDR

In the case of rotationally symmetric bodies, the MDR consists of two simple steps (Popov and Heß, 2014). First, the original three dimensional profile $z = f(r)$ is replaced by the one-dimensional profile $g(x)$ by means of the transformation:

$$g(x) = |x|\int_0^{|x|}\frac{f'(r)}{\sqrt{x^2-r^2}}\mathrm{d}r. \tag{38}$$

This first step is schematically illustrated in Fig. 2. For a sphere with radius R, the shape in the vicinity of the contact

is given by $f(r) = r^2/2R$. In the case of parabolic profile, the transformation (38) again leads to a parabolic profile $g(x)$:

$$f(r) = \frac{r^2}{2R} \Rightarrow g(x) = \frac{x^2}{R}. \tag{39}$$

In the second step, the elastic half-space must be replaced by an elastic foundation consisting of independent springs having normal and tangential stiffnesses

$$k_z = E^* \Delta x, k_x = G^* \Delta x, \tag{40}$$

If the MDR-transformed profile $g(x)$ is indented by the depth d into the elastic foundation, the displacement of individual springs inside the contact will be determined by the equation

$$u_z(x) = d - g(x) = d - \frac{x^2}{R}. \tag{41}$$

For the adhesive contact the boundary springs in contact can be found using the *rule of Heß* (Popov and Heß, 2015). According to this rule the condition of equilibrium of boundary springs (at $x = \pm a$, a being the current contact radius) can be written as

$$\Delta l = \Delta l_{\max}(a) = \sqrt{\frac{2\pi a \Delta\gamma}{E^*}}. \tag{42}$$

Note that this relation is nonlocal as the critical spring displacement Δl depends on a. Combining (41) and (42), we get

$$u_z(a) = d - \frac{a^2}{R} = -\Delta l_{\max}(a) = -\sqrt{\frac{2\pi a \Delta\gamma}{E^*}}. \tag{43}$$

Hence,

$$d = \frac{a^2}{R} - \sqrt{\frac{2\pi a \Delta\gamma}{E^*}}. \tag{44}$$

The normal force can be calculated as a sum of all spring forces:

$$\begin{aligned} F_z(a) &= \int_{-a}^{a} u_z(x)\mathrm{d}x = 2E^* \int_0^a \left(d - \frac{x^2}{R}\right)\mathrm{d}x \\ &= \frac{4E^* a^3}{3R} - \sqrt{8\pi a^3 E^* \Delta\gamma}. \end{aligned} \tag{45}$$

It is convenient to present both analytical and numerical results in dimensionless units:

$$\tilde{a} = \frac{a}{a_0}, \quad \tilde{F}_z = \frac{F_z}{F_0}, \quad \tilde{d} = \frac{d}{d_0}, \tag{46}$$

where F_0, a_0 and d_0 are the critical values of the force, the contact radius and the absolute value of the indentation depth at the moment of detachment of the parabolic profile from the elastic half-space under "controlled force" condition, (Popov and Heß, 2014, 2015):

$$\begin{aligned} F_0 &= \frac{3}{2}\pi R \Delta\gamma, \quad a_0 = \left(\frac{9\pi R^2 \Delta\gamma}{8E^*}\right)^{1/3}, \\ d_0 &= \left(\frac{3\pi^2 R \Delta\gamma^2}{64 E^{*2}}\right)^{1/3}. \end{aligned} \tag{47}$$

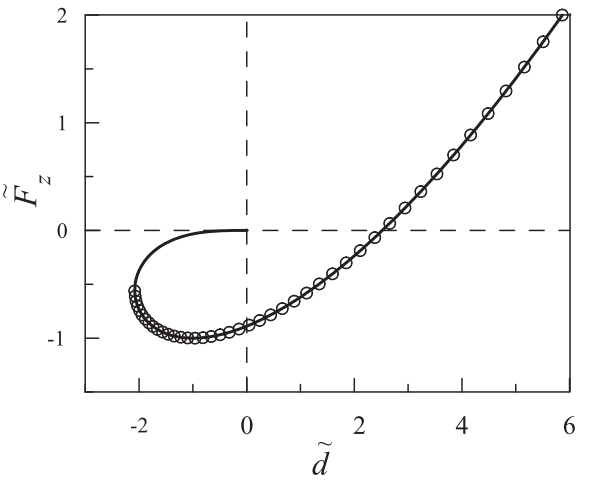

Fig. 3. Dependence on the normal force on the indentation depth for the normal contact with adhesion. Solid line describe analytical solution defined by Eq. (48). Circles represent results of numerical simulations.

In dimensionless variables, Eqs. (44) and (45) take the form

$$\begin{aligned} \tilde{d} &= 3\tilde{a}^2 - 4\tilde{a}^{1/2}, \\ \tilde{F}_z &= \tilde{a}^3 - 2\tilde{a}^{3/2}, \end{aligned} \tag{48}$$

which of course just reproduces the classical solution of Johnson et al. (1971) and can be used to test the numerical model. In Fig. 3 the results of the test are shown. The solid line refer to the dependence given in implicit form in Eq. (48). The circles represent results of the computer experiment. It is obvious that both agree perfectly with each other.

The numerical model is implemented as follows: In every time step first the spring displacements are calculated. Due to the assumption of no slip the displacements of a spring at the position x_i will be given by $\tilde{u}_z(x_i) = u_z - g(x_i)$ and $\mathrm{d}\tilde{u}_x(x_i) = \mathrm{d}u_x + R\mathrm{d}\varphi$. With (43) it is checked whether a spring still remains in contact. After that the new contact radius is calculated. The total contact forces can be calculated easily by summation over all springs in contact at the given time moment: $F_N = E^* \Delta x \sum_{cont} \tilde{u}_z(x_i)$and $F_f = G^* \Delta x \sum_{cont} \tilde{u}_x(x_i)$. Finally the equations of motion (2)–(4) are solved with an explicit Euler method. The parameters that can be changed within the model are R, $E*$, $G*$, m, two components of velocity as well as angular velocity before the impact.

As a second test, we provide a comparison of our numerical results with the ones obtained by Maw et al. (1976) for the oblique impact without adhesion and with no-slip condition. Their results for an infinite coefficient of friction μ should correspond to ours in case of no adhesion, i.e. $\beta = 0$. Maw et al. introduced a dimensionless tangential force

$$\tilde{F}_x^* = \frac{3(1-\nu)F_x}{4C^3 R^2 G\mu} \tag{49}$$

as a function of the dimensionless time $\tilde{t} = t/\tau$, where

$$\tau = \frac{2.9432 C^2 R}{v_{z0}} \tag{50}$$

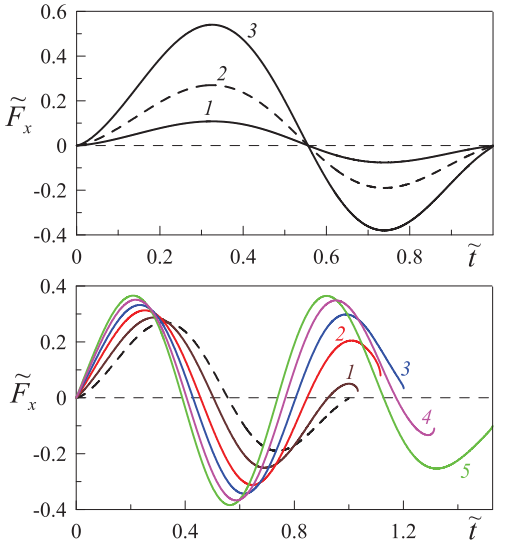

Fig. 4. Dependencies of dimensionless tangential force $\tilde{F}_x$ as a function of dimensionless time $\tilde{t}$, with parameters $R = 0.02$ m, $E^* = 10^{10}$ Pa, $\rho = 1000$ kg/m^3, $\omega_0 = 0$ rad/s, $v_{z0} = 0.01$ m/s, $\nu = 0.3$. Upper panel (case without adhesion): curves 1–3 correspond to the values $\psi = 0.2$, $\psi = 0.5$, $\psi = 1.0$ Bottom panel: $\psi = 0.5$ and surface energies: $\Delta\gamma = 1.0$ J/m^2 , $\Delta\gamma = 5.0$ J/m^2 , $\Delta\gamma = 10.0$ J/m^2 , $\Delta\gamma = 17.0$ J/m^2, $\Delta\gamma = 24.0$ J/m^2 . Dashed line in both panel correspond to non-adhesive case with $\psi = 0.5$.

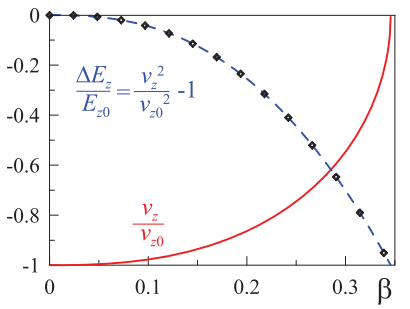

Fig. 5. Dependencies (31) (solid line) and (32) (dashed line) as functions of parameter β (37). The impacts were calculated for various initial conditions, various radii, elastic moduli, masses of the spheres and values of separation energy. Independently of the parameters used, all data collapse to a master curve. The approximation (55) is shown with diamonds.

denotes the duration of the Hertzian impact – and a generalized angle of incidence $\psi*$ (Maw et al., 1976),

$$\psi^* = \frac{2(1-\nu)v_{x0}}{\mu(2-\nu)v_{z0}}. \tag{51}$$

The constant C in (49) and (50) has the form (Maw et al., 1976)

$$C = \left(\frac{15m(1-\nu)v_{z0}^2}{16GR^3}\right)^{1/5}. \tag{52}$$

It is obvious from the definitions (49) and (51) that the limiting case $\mu \to \infty$ of the dependence $\tilde{F}_x^* = \tilde{F}_x^*(\psi^*)$ cannot be studied directly. However, when looking at the results of Maw et al. it can be noticed, that for small values of $\psi*$, i.e. dominance of the stick regime, this dependence can be written in the approximate form

$$\tilde{F}_x^*(\psi^*,\ \tilde{t}) \approx \psi^* \tilde{F}_x^*(\psi^* = 1,\ \tilde{t}). \tag{53}$$

Hence, the results will almost not be changed by the transformations

$$\begin{aligned} &\tilde{F}_x^* \to \mu \tilde{F}_x^* \equiv \tilde{F}_x, \\ &\psi^* \to \mu \psi^* \equiv \psi. \end{aligned} \tag{54}$$

Using these variables, the case without slip can be studied without problems as the coefficient of friction does not appear at all.

In Fig. 4, we plotted the tangential force variation during the impact. In the upper panel the results of Maw et al. are reproduced. Thereby, the curves 1, 2 and 3 correspond to the different values of ψ. The lower panel of Fig. 4 gives the corresponding results of our calculations with adhesion for different values of the surface energy $\Delta\gamma$. It can be seen, that the curves for small surface energies tend towards the case without adhesion. Moreover, the impact duration as well as the frequency and amplitude of the tangential force oscillation is increased with increasing surface energies. The ends of all lines correspond to the time just before detachment. Note that in the non-adhesive case last value of force at the time of detachment is $\tilde{F}_x = 0$, whereas in the case of adhesion it is $\tilde{F}_x \neq 0$ at the end of contact. The value of the normal force at detachment is also nonzero in the adhesive case (see Fig. 3).

5. Results of modeling

The results for the dimensionless rebound velocity v_z/v_{z0} together with the loss of kinetic energy of vertical motion $\Delta E_z/E_{z0}$ during the impact as a function of the parameter β are presented in Fig. 5. They can be approximated by the function

$$\begin{aligned} \frac{\Delta E_z}{E_{z0}} \approx &-0.0019\sqrt{\beta} + 0.0413\beta - 2.7194\beta^2 - 24.2169\beta^3 \\ &+ 30.073\beta^4 - 23.5737\beta^5 \end{aligned} \tag{55}$$

from which the rebound velocity v_z can be calculated with (31) and (32). The coefficient of determination for approximation (55) and the numerical dependency in the full range is $R^2 > 0.99999997$.

The results for the dimensionless rebound velocities $\frac{7}{2}\frac{v_x - \tilde{v}_x}{V} = \frac{7}{5}\frac{R(\omega - \tilde{\omega})}{V} = P(\gamma, \beta)$ as well as the loss of kinetic energy of horizontal motion during the impact are given in Fig. 6 as functions of the parameter γ. The numerical calculations have been done for $\beta = 0$, $\beta = 0.2$ and $\beta = 0.3$. Note that if the bodies have equal Poisson numbers: $\nu_1 = \nu_2 = \nu$, then $G^*/E^* = 2(1-\nu)/(2-\nu)$. It is $-1 < \nu \leq 1/2$, due to thermodynamic stability restrictions (Landau and Lifshitz, 1970). Thus, for isotropic bodies, $2/3 < G*/E* < 4/3$ which corresponds to $1.52 < \gamma < 2.16$. However, for anisotropic (e.g. orthotropic) media, the effective ratio $G*/E*$ can be in a wider range. We therefore present results outside this interval as well. The range for isotropic bodies is marked by vertical dotted lines. Dependences of the dimensionless rebound velocities and the loss of kinetic energy of

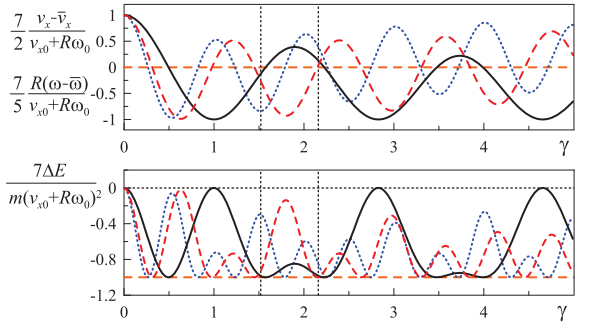

Fig. 6. The variables $\frac{7}{2}\frac{v_x-\bar{v}_x}{V}$, $\frac{7}{5}\frac{R(\omega-\bar{\omega})}{V}$ and $\frac{7\Delta E_x}{m(v_{x0}+R\omega_0)^2}$ as functions of the parameter $\gamma=\sqrt{(7/2)(G^*/E^*)}$. The impacts were calculated for various initial conditions, various radii, elastic moduli and masses of the spheres. Independently of the parameters used, all data collapse to a master curve. The classical rigid-body solution (6, 7) is shown by the horizontal dashed line. Solid lines correspond to $\beta=0$, dashed lines to $\beta=0.2$ and dotted lines to $\beta=0.3$.

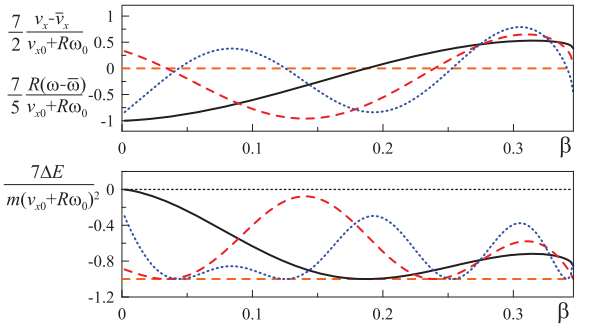

Fig. 7. Dependencies of the variables shown in Fig. 6 on the parameter β (37). Solid lines correspond to $\gamma=1$, dashed lines to $\gamma=2$ and dotted lines to $\gamma=3$.

horizontal motion as functions of the parameter β are presented in Fig. 7.

Note that the critical value of the parameter β is $\beta_c\approx 0.34582$. If $\beta>\beta_c$ the sphere reaches an idle state with $u_z<0$ and $v_z=0$ while due to adhesion it is still in contact with the half space. In this case, the particle remains stuck on the substrate. The same effect is observed in the linear model (16), where the particle remains stuck if $\frac{d_c}{v_{z0}}\sqrt{\frac{k_z}{m}}>1$. In the following we will only investigate the "rebound region" corresponding to $\beta<\beta_c$.

The full dependence $P(\gamma,\beta)$ is shown in Fig. 8. In the top panel the 3D surface $P(\gamma,\beta)$ is shown, in the bottom panel the respective map of the heights.

Within the interval $1.52<\gamma<2.16$ the numerical solution $P(\gamma,\beta)$ can be approximated by the formula

$$P(\gamma,\beta)\approx a_0+a_1\gamma+a_2\gamma^2+a_3\gamma^3+a_4\gamma^4, \tag{56}$$

with coefficients a_i depending of the second parameter β:

$$\begin{aligned}a_0 &= 43.139-1171.292\beta+26272.84\beta^2-425164.358\beta^3\\ &\quad+2019578.141\beta^4-2730636.482\beta^5,\end{aligned}$$

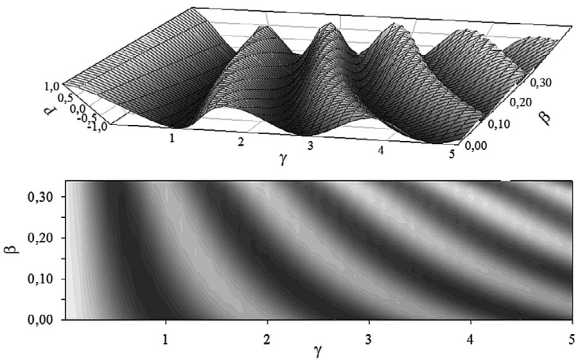

Fig. 8. Top panel: 3D dependency $P(\gamma,\beta)$ (29); Bottom panel: 2D dependency $P(\gamma,\beta)$ (29), in which value is shown by gradient intensity.

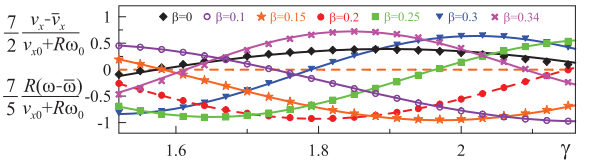

Fig. 9. Comparison between the numerical results (solid lines) and their approximation (56) for the solution $P(\gamma,\beta)$ as a function of $\gamma=\sqrt{(7/2)(G^*/E^*)}$.

$$\begin{aligned}a_1 &= -107.979+2330.636\beta-59003.404\beta^2\\ &\quad+973668.408\beta^3-4542494.427\beta^4+6011602.434\beta^5,\\ a_2 &= 95.513-1659.826\beta+49929.478\beta^2-830694.428\beta^3\\ &\quad+3787497.609\beta^4-4889171.548\beta^5,\\ a_3 &= -35.686+507.716\beta-18909.789\beta^2+312224.871\beta^3\\ &\quad-1384531.709\beta^4+1737264.447\beta^5,\\ a_4 &= 4.786-57.27\beta+2693.537\beta^2-43475.09\beta^3\\ &\quad+186768.848\beta^4-227031.806\beta^5.\end{aligned} \tag{57}$$

These approximations are shown together with the computer experiment results in Fig. 9. It can be seen that the approximation describes well the numerical results for all relevant values of both determining parameters of the problem. The biggest difference between the approximation and the experimental data is observed at the boundaries $\beta\approx 0$ and $\beta\approx\beta_c$.

Note that the functions $P(\gamma,\beta)$ and $F(\beta)$ provide the complete solution of the examined impact problem. For example, we can find the rebound angle β° as a function of the grazing angle α°. According to Fig. 1 we have $\tan\alpha^\circ=v_{z0}/v_{x0}$ and $\tan\beta^\circ=|v_z|/v_x$. From Eqs. (29) and (31) we can calculate

$$\tan\beta^\circ=\frac{7F(\beta)}{2}\left(\frac{2P(\gamma,\beta)+5}{2\tan\alpha^\circ}-\frac{R\omega_0(P(\gamma,\beta)+1)}{v_{z0}}\right)^{-1}. \tag{58}$$

From the last formula, we can see that in case of $\omega_0\neq 0$ the rebound angle depends on the initial velocity v_{z0}. For

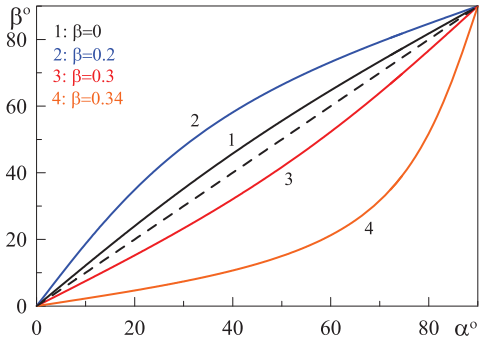

Fig. 10. Rebound angle β° as a function of grazing angle α° (59) for $\gamma = 1.8$ and different values of parameter β (37). Curves 1–4 correspond to values $\beta = 0,\ 0.2,\ 0.3$ and 0.34, respectively. Dashed line denotes the bisector $\alpha^\circ = \beta^\circ$.

$\omega_0 = 0$ (58) can be written in the simpler form

$$\tan\beta^\circ = \frac{7F(\beta)\tan\alpha^\circ}{2P(\gamma,\beta)+5}. \tag{59}$$

Note again that the absence of adhesion corresponds to $F(\beta) \equiv 1$. In Fig. 10 the relation (59) is shown for several different parameters of the model. Fig. 11 gives the full dependence of the rebound angle as a function of the grazing angle and the parameter γ for different values of the parameter β.

6. Comparison with experimental results

As it was pointed out before, no efforts – neither analytical, numerical nor experimental – have yet been published, to our knowledge, to discuss the full plain adhesive impact problem. Nevertheless several papers analyze the pure normal adhesive contact. Dahneke (2007) gave experimental results for particle-surface collisions for spherical particles from polystyrene. In Fig. 12 a comparison is shown between these and our calculations. The experimental results do not converge to the value 1. Dahneke argues that this is due to non-elastic effects in the material. That's why we also normalized our values in the figure on the non-elastic limiting value 0.96 to exclude the effects which are not considered in our model. It is obvious, that the agreement between numerical and experimental results is very good.

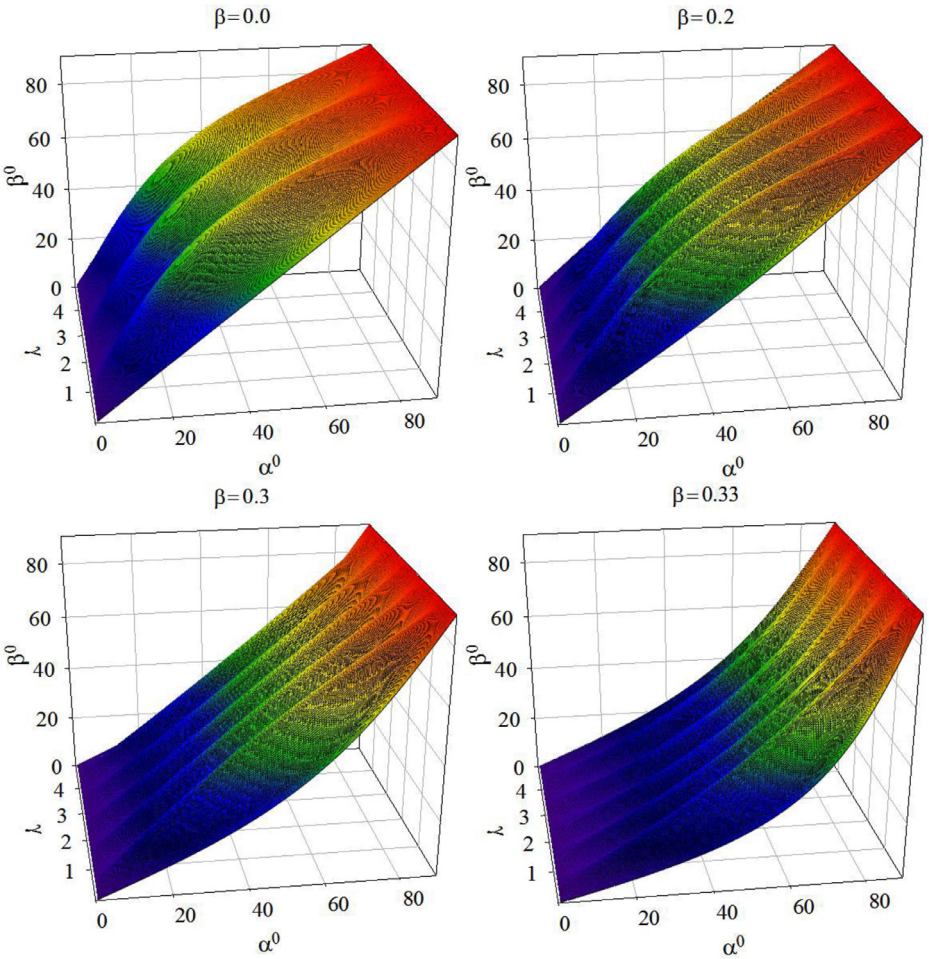

Fig. 11. Rebound angle β° as a function of grazing angle α° and $\gamma = 0 \ldots 5$ for different values of β (37).

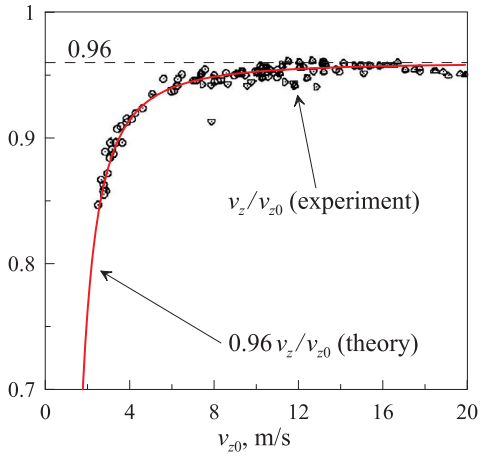

Fig. 12. Comparison between experimental results by Dahneke (2007) and numerical results (red line) at parameters $R = 0.635 \cdot 10^{-6}$ m, $\rho = 1000$ kg/m^3, $E = 3 \cdot 10^9$ Pa, $\Delta\gamma = 0.15$ J/m^2. These are normalized by the factor 0.96 to exclude non-elastic effects in the material which are not considered in the model.

7. Conclusions

In the present paper, we used the method of dimensionality reduction in the area of its exact applicability (contact of axis-symmetric bodies) to calculate the impact between a sphere and an elastic half space with adhesion under no slip condition. The influence of adhesion was described by the theory of Johnson, Kendall and Roberts (JKR-theory), the results of which can be reproduced exactly by the described numerical method.

It was shown, that the adhesive properties of the impact can be described by single dimensionless parameter. In Lyashenko and Popov (2015) it was already shown, that the elastic properties of the impact can be described completely by the Mindlin-ratio. The rebound velocities after the impact as functions of the two mentioned parameters have been calculated and an analytical approximation for the numerical results has been given.

Acknowledgments

This work was supported in part by Tomsk State University Academic D.I. Mendeleev Fund Program and the Deutsche Forschungsgemeinschaft.

References

Andres, R.P., 1995. Inelastic energy transfer in particle/surface collisions. Aerosol Sci. Technol. 23, 40–50.
Borodich, F.M., Galanov, B.A., Prostov, Y.I., Suarez-Alvarez, M.M., 2012. Influence of complete sticking on the indentation of a rigid cone into an elastic half space in the presence of molecular adhesion. J. Appl. Math. Mech. 76, 590–596.
Brilliantov, N.V., Albers, N., Spahn, F., Pöschel, T., 2007. Collision dynamics of granular particles with adhesion. Phys. Rev. E 76, 051302.
Brilliantov, N.V., Spahn, F., Hertzsch, J.-M., Pöschel, T., 1996. Model for collisions in granular gases. Phys. Rev. E 53, 5382–5392.
Campañá, C., Persson, B.N.J., Müser, M.H., 2011. Transverse and normal interfacial stiffness of solids with randomly rough surfaces. J. Phys.: Condens. Matter 23, 085001.
Ciamarra, M.P., Lara, A.H., Lee, A.T., Goldman, D.I., Vishik, I., Swinney, H.L., 2004. Dynamics of drag and force distributions for projectile impact in a granular medium. Phys. Rev. Lett. 92, 194301.
Dahneke, B., 2007. Particle bounce or capture – search for an adequate theory: i. conservation-of-energy model for a simple collision process. Aerosol Sci. Technol. 23, 25–39.
Grzemba, B., Pohrt, R., Teidelt, E., Popov, V.L., 2014. Maximum micro-slip in tangential contact of randomly rough self-affine surfaces. Wear 309, 256–258.
Hertz, H., 1881. Über die Berührung fester elastischer Körper. J. für die reine Angew. Math. 92, 156–171.
Hunter, S.C., 1957. Energy absorbed by elastic waves during impact. J. Mech. Phys. Solids 5, 162–171.
Johnson, K.L., Kendall, K., Roberts, A.D., 1971. Surface energy and the contact of elastic solids. Proc. R. Soc. A 324, 301–313.
Jop, P., Forterre, Y., Pouliquen, O., 2006. A constitutive law for dense granular flows. Nature 441, 727–730.
Kosinski, P., Hoffmann, A.C., 2011. Extended hard-sphere model and collisions of cohesive particles. Phys. Rev. E 84, 031303.
Landau, L.D., Lifshitz, E.M., 1970. Theory of Elasticity. Pergamon Press.
Ledvinkova, B., Kosek, J., 2013. The effects of adhesive forces on the collision behavior of polyolefin particles. Powder Technol. 243, 27–39.
Lyashenko, I.A., Popov, V.L., 2015. Impact of an elastic sphere with an elastic half space revisited: numerical analysis based on the method of dimensionality reduction. Sci. Rep. 5, 8479.
Maw, N., Barber, J.R., Fawcett, J.N., 1976. The oblique impact of elastic spheres. Wear 38, 101–114.
Maw, N., Barber, J.R., Fawcett, J.N., 1977. The rebound of elastic bodies in oblique impact. Mech. Res. Commun. 4, 17–22.
Maw, N., Barber, J.R., Fawcett, J.N., 1981. The role of elastic tangential compliance in oblique impact. J. Lubr. Technol. 103, 74–80.
Popov, V.L., 2013. Method of reduction of dimensionality in contact and friction mechanics: a linkage between micro and macro scales. Friction 1, 41–62.
Popov, V.L., Heß, M., 2014. Method of dimensionality reduction in contact mechanics and friction: a users handbook. I. Axially-symmetric contacts., 12. Series Mechanical Engineering, Facta Universitatis, pp. 1–14.
Popov, V.L., Heß, M., 2015. Method of dimensionality reduction in contact mechanics and friction. Springer ISBN 978-3-642-53875-9.
Popov, V.L., Psakhie, S.G., 2007. Numerical simulation methods in tribology. Tribol. Int. 40, 916–923.
Thornton, C., Yin, K.K., 1991. Impact of elastic spheres with and without adhesion. Powder Technol. 65, 153–166.
Waters, J.F., Guduru, P.R., 2009. Mode-mixity-dependent adhesive contact of a sphere on a plane surface. Proc. R. Soc. A 466, 1303–1325.